In-depth analysis of Lime-hemp concrete and water vapor interactions: Effect of water default and prediction of the sorption behavior

Brahim Mazian, Giana Almeida, Nils Frantz, Patrick Perré

In-depth Analysis of Lime-Hemp Concrete and Water Vapor Interactions: Effect of water default and prediction of the sorption behavior

Brahim Mazian[1*], Giana Almeida[2], Nils Frantz[1], Patrick Perré[1,3]

[1]Université Paris-Saclay, CentraleSupélec, Laboratoire de Génie des Procédés et Matériaux, Centre Européen de Biotechnologie et de Bioéconomie (CEBB), 3 rue des Rouges Terres 51110 Pomacle, France.

[2]Université Paris-Saclay, INRAE, AgroParisTech, UMR SayFood, 91120, Palaiseau, France.

[3]Université Paris-Saclay, CentraleSupélec, Laboratoire de Génie des Procédés et Matériaux, 3 rue Joliot Curie, 91190 Gif-sur-Yvette, France.

*Corresponding author

Brahim.mazian@centralesupelec.fr

Graphical abstract

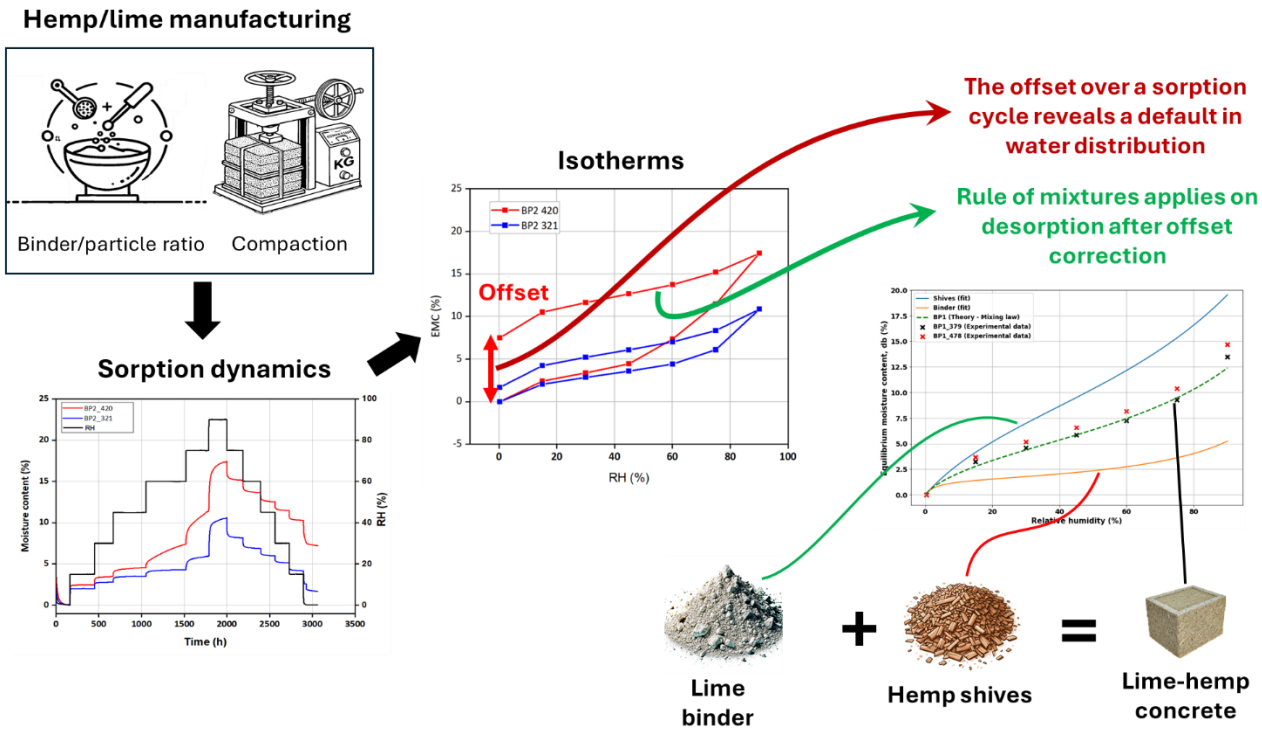

Abstract

Lime-hemp concrete (LHC) emerges as a sustainable building material due to its low embodied energy, carbon storage capabilities, and interesting properties for both winter and summer comfort. However, a comprehensive understanding of its moisture behavior is pivotal for its development and application in construction. This study investigates the moisture sorption behavior and isotherm characteristics of LHC across four formulations varying in density (321–478 kg/m³) and binder/particle weight ratios (BP = 1 and 2). Using a strict equilibrium criterion, over 3000 hours of Dynamic Vapor Sorption (DVS), experiments revealed some formulations failed to reach equilibrium during adsorption at RH levels above 60%, indicating irreversible processes characterized by offsets in equilibrium moisture content (EMC) at 0% RH after a complete cycle. These phenomena were attributed to insufficient water availability during mixing and/or excessive compaction. Formulations with a higher weight ratio (B/P=2) and significant compaction, such as BP2_420, exhibited the highest desorption offset (7.5% EMC), while those with a lower B/P weight ratio (B/P=1), such as BP1_379, showed reduced offsets below 2%, due to better water distribution. The study also showed that reversible sorption behavior, corrected for offsets, could be accurately described using the Guggenheim-Anderson-de Boer (GAB) model. Finally, the rule of mixtures reliably predicted sorption isotherms by combining the GAB parameters of hemp shive particles and binders, with deviations limited to a maximum error of 2.3%.

Keywords: sorption; lime-hemp concrete; hysteresis; water-availability, rule of mixtures

1. Introduction

The construction sector accounts for approximately 40% of global energy use and material resource consumption, contributing significantly to greenhouse gas emissions [1,2]. This is why this sector is under strong pressure to respond to global environmental concerns, in order to reduce the sector's carbon footprint and resource consumption. To mitigate these impacts, there is a growing shift towards developing and adopting eco-friendly building materials, including bio-based alternatives that can offer lower embodied energy compared to traditional construction materials. Among these innovations, vegetable concrete has emerged as a promising solution, combining the thermal insulation and moisture regulation properties of plant-based aggregates, such as hemp or flax, with the structural capabilities of mineral binders [3]. This synergy not only ensures good thermal performances but also enhances indoor comfort through improved hygrothermal properties [4]. These benefits make bio-based concretes a distinctive alternative to conventional building materials, addressing both ecological and economic challenges within the construction sector [5,6].

Lime-hemp concrete (LHC), commonly known as hempcrete, is one of the most promising bio-based concretes due to its technical, environmental, and economic benefits [7,8]. While traditional concrete includes coarse aggregates, the term "concrete" in LHC refers to its composite nature and application in construction. The versatility of LHC makes it suitable for a wide range of walls, floors, and roofs in both new construction and renovation [9]. Despite its relatively low compressive strength generally, requiring the integration of auxiliary structural supports to provide load-bearing walls, the LHC's remarkable hygrothermal behavior makes it possible to envisage massive development [10,11]. With thermal conductivity ranging between 0.06 and 0.16 $W.m^{-1}.K^{-1}$, it serves as an effective insulator, potentially eliminating the need for additional insulation layers [12,13]. Like other plant-based materials, LHC is an efficient humidity regulator thanks to its pronounced adsorption and desorption characteristics [4,14].

These properties enable LHC to stabilize indoor humidity levels by absorbing excess moisture when the humidity is high and releasing it back into the environment when conditions are drier. This dynamic moisture regulation capability not only mitigates the risk of condensation within the building structure but also plays a crucial role in preserving air-indoor quality [15]. Additionally, LHC's hygroscopic behavior enhances summer comfort by increasing thermal inertia through latent heat exchange over daily variations of external conditions (temperature and relative humidity), further boosting its suitability for modern, sustainable construction [4,16].

However, previous studies have highlighted the critical influence of moisture content on the heat and moisture transfer and storage dynamics of bio-based materials like hemp concrete [14,17,18]. Therefore, a thorough understanding of moisture content fluctuations within LHC is essential for accurately characterizing its hygrothermal behavior in response to environmental changes. Experimental data on the hygroscopic properties of hemp concrete remain somewhat limited and show considerable variability across different investigations. Moreover, the methodologies and parameters employed for the hygroscopic characterization of hemp concrete differ and are the subject of ongoing discussion [19]. Traditional methods for determining sorption isotherms (equilibrium moisture content, EMC, as a function of relative humidity of the air, RH), as outlined in standards such as NF EN ISO 12571, often rely on saturated salt solutions or climatic chambers [4,20,15,17]. While these methods are widely accepted, they have faced criticism for their labor-intensive nature and potential inaccuracies. Recent research has shifted towards dynamic vapor sorption (DVS) with enhanced efficiency and precision [17,21], provided the equilibrium criterion is demanding.

Numerous studies have been conducted to investigate the hygroscopic behavior of hemp concrete. For instance, one study demonstrated that LHC, with binder-to-hemp and water-to-hemp weight ratios of 1.2 and 2.38, respectively, reached a moisture content of approximately

16% at 90% relative humidity (RH) [22]. Sorption hysteresis has also been reported in several works, attributing these findings to mechanisms such as capillary condensation hysteresis, contact angle hysteresis, and the ink-bottle effect, depending on the combination of pore sizes present and RH applied [15,22,23]. Note that the sorption hysteresis, always observed in lignocellulosic materials, is attributed to the effect of sorption history on the macromolecular conformation [24,25] rather than explanations involving liquid water, as this process occurs in the domain of bound water. All previous phenomena, more related to capillary condensation, can only explain the upper part of the sorption isotherm [26]. It is important to remember that sorption hysteresis is defined as the gap between the two envelop curves obtained during sorption cycles. During a cycle, these envelop curves pass through the origin (EMC = 0 at RH = 0). The situation is more complex when the offset observed at RH = 0 after one cycle reveals an irreversible mass uptake. A study examined three types of hemp concrete with different compositions and manufacturing methods: precast, sprayed, and molded [4]. Their results showed variations in sorption capacity, hysteresis, and irreversibility (offset after a full cycle: adsorption until 97 % RH followed by desorption to 0 % RH). In particular, the authors observed a significant irreversible mass in sprayed and molded hemp concrete compared to precast variants. Another study confirms the presence of hysteresis phenomena accompanied by an irreversible portion of desorption [27]. This could be due to the carbonation reaction of the binder at a high RH level [4].

Research was also carried out to compare hemp concretes with identical formulations but varying compaction levels [28]. Their findings revealed that the most densely compacted sample demonstrated increased equilibrium moisture content at every RH level. They attributed these results to a higher presence of mesopores for the denser mixture, which is a consequence of the applied compaction stresses. These pore sizes tend to increase adsorption by capillary condensation within the material. In fact, capillary condensation occurs in small pores, and

according to the Kelvin equation, only pores with a radius larger than 96 nm will remain empty at 98.9% RH [26]. This suggests that the denser samples contain a significant number of mesopores smaller than this threshold, contributing to the increased EMC observed at higher RH. In addition to empirical investigations, some efforts have been dedicated to developing numerical models to predict hygrothermal properties, mainly focusing on hysteresis effects between adsorption and desorption phases [29,14,30]. These models show that ignoring hysteresis can lead to inaccurate predictions. For example, Derluyn et al. [29] found that neglecting hysteresis in concrete can underestimate durability risks, while Oumeziane et al. [14] and Rémond et al. [31] demonstrated that including hysteresis in biosourced materials is needed to predict the moisture buffering effect accurately.

While various results concerning the sorption of vegetable concrete have been reported in the literature, the correlation between the composition of pure components of LHC, its post-processing factors like compaction, and its sorption behavior (notably hysteresis and irreversibility, which are crucial for LHC performance) remains largely unexplored. Moreover, the theoretical approach traditionally used to predict the properties of composite materials from their individual components has not been applied to LHC. By integrating this approach, the present study offers novel insights into the interplay between the constituents of LHC and their collective impact on its hygroscopic behavior.

Accordingly, this study investigates the sorption phenomena and isotherm characteristics of LHC by examining four contrasted formulations, as well as their individual components (binder and particle). The selected formulations vary in binder/particle weight ratio (B/P), with ratios of 1 (BP1) and 2 (BP2), and in compaction, resulting in different densities. This work relies on DVS measurements using a very strict equilibrium criterion, which turned into a full sorption-desorption cycle of more than 3000 hours. To the best of our knowledge, this represents the first instance of such an extended dynamic sorption experiment being conducted on this type of

material. These extensive tests provide a unique dataset for detailed analysis of hysteresis and irreversibility effects to clarify the mechanisms of moisture interaction in these materials. Furthermore, the study proves that the rule of mixtures applies to the reversible part of the sorption isotherm, which allows the properties of the composite materials to be predicted by their individual components.

2. Materials and method

2.1. Raw materials

LHC samples assessed in this research were manufactured using a lime binder, hemp shive particles, and a water-retaining agent (Hydroxypropyl-Methyl Cellulose). The hemp shives, provided by Agrochanvre in Normandy, France, were harvested in September 2021, featuring lengths ranging from 1 to around 40 mm and widths from 0.5 to 5 mm. The particle's sizes were measured by image analysis (ImageJ version 1.53) and are shown in **Fig 1.** Over 1000 particles were analyzed, providing detailed data [11]. These shives possess a bulk density of roughly 100 $kg.m^{-3}$ according to the supplier and an apparent density of about 300 $kg.m^{-3}$. The binder used in the concrete mix was Tradical® Thermo, comprising approximately 80% air lime and 20% cement. HydroxyPropyl Methyl Cellulose (HPMC), sourced from DEFI - Houillères de Cruéjouls, was added to the mix as an additive at a 2% weight-to-weight ratio relative to the mixing water, aiming to improve the mixture's stability by reducing mass mobility.

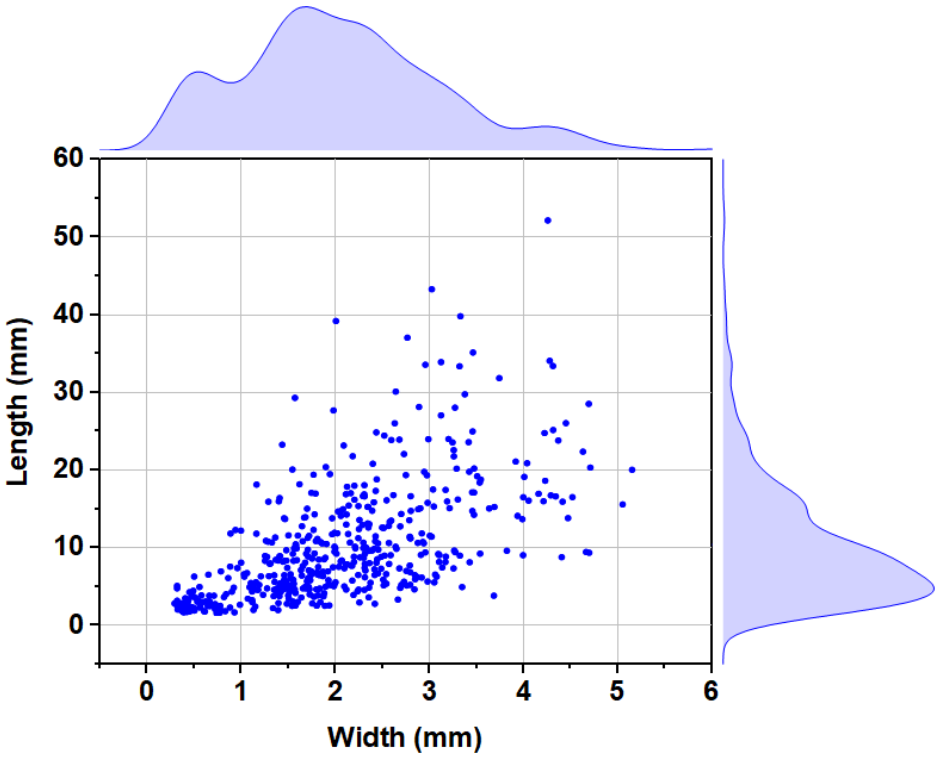

Fig. 1. Hemp shive particles geometric analysis: scatter plot and side distributions of width and length, weighted by particle size.

2.2.Materials processing

Following the experimental design outlined by Frantz et al. [11], this study focused on materials within the "Raw" category (composed of "building" certified hemp particles, in bulk, directly from Agrochanvre's processes). First, the hemp particles were pre-wetted with 170% water relative to their mass (with a moisture content of 12%, dry basis) for 5 minutes in a horizontal shaft mixer (manufactured by 3R) (**Fig 2a).** In parallel, the binder was prepared by mixing 40% (w/w) water with an additional 20% water relative to the particle mass to compensate for water absorption by the hemp particles. The water-retaining agent (HPMC, 2 % w/w) was added to this mixing water using a standard kitchen mixer. The binder-water mixture was then added to the pre-wetted hemp particles, and everything was mixed for an additional 8 minutes. The target densities for the hemp concrete were achieved by precisely measuring all components with a precision scale (Minebea Intec) and molding the mixture into 15 × 15 × 15 cm^3 cubes, in

accordance with the NF EN 12 390–3 standard **(Fig 2b-c)**. The required quantity of mixture was manually compacted to fit the molds volume. For the denser sample (BP1), with a target density of 478 kg/m³, a hydraulic press was needed to reach the required compaction. To ensure homogeneity, each cube was compacted into three layers of 5 cm, and a metal plate was placed on top to evenly distribute the pressure. Demolding occurred 30 minutes after compaction, sufficient to maintain the cubic shape of the specimens and ensure their cohesion and stability. After demolding, all materials were initially stored at 70% relative humidity and 20°C for 48 hours, then transferred to ambient conditions (20°C and 50% relative humidity) for stabilization over approximately one year. (**Fig. 2b-c**).

Additionally, a control cube, composed solely of hydrated binder (Tradical® Thermo product), was prepared with 40% (w/w) water and compacted to reach a density of 1,300 kg/m³, according to the manufacturer's specifications. Four material configurations, named BP1-379, BP1-478, BP2-321, and BP2-420 (**Table 1)**, were selected in the present work to separate the effects of B/P ratios and density on sorption behavior while retaining configurations suitable for insulated walls.

Table 1. Apparent density, binder/particle ratio (weight/weight), and proportion of mixed materials.

Samples	Binder (g)	Particles (g)	Water (g)	Binder/Particle (B/P)	Apparent density ($kg.m^{-3}$)
BP1-379	579	579	347	1	379
BP1-478	723	723	434	1	478
BP2-321	552	276	276	2	321
BP2-420	736	368	368	2	420

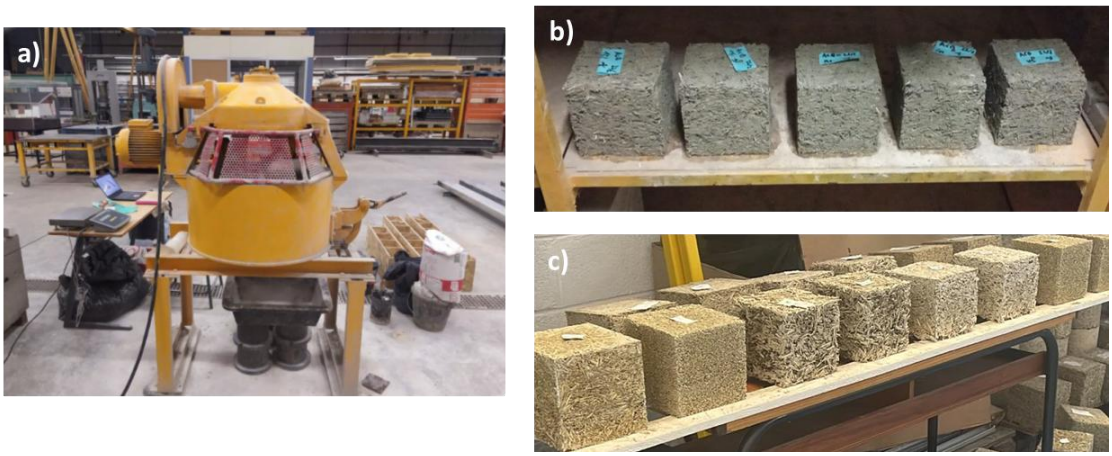

Fig. 2. (a) Shaft Mixer used in mixing stage, (b) conditioning in a climatic chamber (70% RH, 20°C), and (c) conditioning at ambient conditions.

To perform the sorption tests, small samples was cut from each LHC cube using a saw. This section was then ground using a hammer to obtain a representative powder sample of approximately 1 g for analysis. Similarly, 1-g samples of the pure components, hemp shive particles and hydrated binder, were also prepared for analysis.

2.3. Water vapor sorption

The sorption tests were conducted using dynamic vapor sorption (DVS) (ProUmid GmbH & Co. KG, Ulm, Germany) equipped with a 23-slot tray. This instrument is a cutting-edge, fully automated system designed for assessing the water vapor sorption of several samples within a controlled temperature and RH environment. The device offers a gravimetric accuracy of 0.1 µg for samples up to 22 g, which is the case of samples used in this study. An internal mass reference corrects any microbalance drift, ensuring outstanding balance stability, even during prolonged measurements.

Sorption isotherms were measured at 25 ± 0.1°C, under nitrogen flow, with RH levels ranging from 0 to 90 %, by steps of 15 %, and then back to 0 %, by steps of -15 %. The measurement procedure starts with obtaining the sample's dry weight (equilibrium mass at 0% RH). Then, the desired humidity level is set, and changes in the sample's weight are recorded every 20 minutes. Equilibrium in a dynamic sorption experiment is defined as the time at which the mass

derivative is less than the set criterion. In this study, this criterion (dm/dt) was set at 0.0001% per 200 minutes, which is very demanding. With this stringent criterion, each RH step required a minimum of 3000 minutes and a maximum of 330 hours for the samples to reach equilibrium. Upon reaching equilibrium, the subsequent humidity step was initiated.

The sorption tests were performed in duplicate for each sample, ensuring reproducibility and accuracy of the sorption measurements. Data analysis and figure production were done using in-house Python scripts. For all samples, equilibrium moisture content values (EMC, dry basis) were determined using the mass average over the last fifteen data of each RH step.

2.4.GAB model

The GAB model (Eq. 1) was employed to fit the sorption isotherms of LHC due to its well-established applicability for characterizing moisture sorption isotherms in porous and hygroscopic materials. The GAB model extends the widely used BET model, enabling the description of sorption behavior across a broader range of relative humidity (0–90%), making it ideal for this study. This model was applied for adsorption after calculating the moisture content at each humidity level using the initial dry mass equilibrated at 0 % RH. For desorption, to correct for the irreversible residual mass (offset after a complete sorption cycle), the moisture content was calculated using the mass obtained after desorption at 0 % RH as the dry mass. The model parameters were adjusted to fit the experimental data using a Python script, based on the Root Mean Square Error (RMSE) (Eq. 2). Finally, the SEE function was also employed to evaluate the capability of the GAB model in fitting the experimental data points.

$$EMC = \frac{MC_m . C . k . RH}{(1 - k . RH) . (1 - RH + C . k . RH)} \quad \textbf{Eq. (1)}$$

Where EMC is the equilibrium moisture content, MC_m represents the monolayer moisture content ($kg_{water}/kg_{dry\ mass}$) or as a percentage (%), RH is the relative humidity of the air (%), C

is the GAB constant and related to the heat of sorption of the first layer and k is another GAB constant associated with the heat of sorption for the multilayer.

$$\boldsymbol{RMSE} = \sqrt{\frac{\mathbf{1}}{\boldsymbol{N}}\sum_{\boldsymbol{i=1}}^{\boldsymbol{N}}(\boldsymbol{EMC_{exp}} - \boldsymbol{EMC_{pred}})^{\mathbf{2}}} \quad \text{Eq. (2)}$$

$$\mathbf{SEE} = \sqrt{\frac{\sum_{\boldsymbol{i=1}}^{\boldsymbol{N}}\left(\boldsymbol{EMC_{exp}} - \boldsymbol{EMC_{pred}}\right)^{\mathbf{2}}}{\boldsymbol{d_f}}} \quad \text{Eq. (3)}$$

Where N is the number of data points; EMC_{exp} the experimental equilibrium moisture content (% d.b) and EMC_{pred} the equilibrium predicted moisture content (% d.b), df is the degree of freedom, defined as N- p, where p is the number of the parameter in the model.

2.5. Additivity of the sorption behavior

The principle of additivity, also known as the rule of mixtures, was applied to predict the sorption isotherms for mixtures, based on the sorption behaviors of the individual pure components. The objective was to test the prediction of the LHC sorption isotherm by an average weighted by the mass fraction of the constituents isotherms. More clearly, the EMC of the composite at each RH value is computed as the weighted average, by the mass ratio, of the respective EMC values of lime and hemp obtained by the GAB curves at this RH value.

To validate the rule of mixtures, the sorption isotherms for the individual components, shives and hydrated binder (Tradical® Thermo) were then established in addition to the tests on the materials.

3. Results and discussion

3.1. Raw data: sorption dynamics and sorption isotherms

Fig. 3 depicts the moisture dynamics of the tested samples at varying relative humidity (RH) levels. As can be seen, some samples, including the (hydrated) binder, fail to reach the equilibrium state (defined at dm/dt < 0.0001 %/200 min) during adsorption at the highest RH levels, even after several hundred hours, especially above 60 % RH **(Fig. 3c)**. In contrast, equilibrium is always reached in desorption. This difference in behavior between adsorption and desorption, observed for hydrated binder and some LHC formulations **(Fig. 3b and c)**, reveals an irreversible process, confirmed by the offset observed at 0 % RH after a complete cycle.

A very high offset is observed for formulation BP2_420 (exceeding 7 %), whereas formulations BP1_478, BP1_379, and BP2_321 exhibit lower offsets, ranging between 2 % and 3 %. These observations suggest several complex interactions between humidity and the material's physicochemical composition, potentially influenced by the water-to-binder ratio and compaction effects. This explanation is confirmed by the fact that this irreversible behavior is observed at high RH, at values not seen by the material during its storage after manufacturing.

The manufacturing method consisted of adding 40 % water to the binder relative to its mass (the manufacturer’s minimum recommendation), to which 20 % extra water (percentage of particle mass) was added to avoid consumption of setting water by particles. Two percent water-retaining agent (HPMC) was introduced into the mixing water before its incorporation with the binder. Following that, the blend was thoroughly mixed with pre-wetted particles. This process was designed to reduce water mobility and thus minimize setting problems. Nevertheless, considering the water-retaining capacity of hemp shive particles, it is probable that a portion of this extra water remains accessible to the binder. Consequently, binders in formulations with a B/P=1 ratio may potentially receive more water compared to those with a B/P=2 ratio.

Additionally, compaction, while crucial for achieving the desired material density, can induce a non-uniform moisture distribution within the material [14]. Indeed, high compaction may lead to local drainage of water from highly compacted zones, potentially resulting in incomplete dispersion and interaction of the lime binder in these areas. Furthermore, compaction reduces porosity, which may limit the diffusion of CO_2 required for air-lime carbonation [32,33], particularly at relative humidity levels between 50 % and 70 % [34]. Reduced porosity also restricts water retention and storage within the matrix [14], which is critical for maintaining the hydration and carbonation processes.

These hypotheses corroborate the sorption dynamics **(Fig. 3)** and sorption isotherm curves **(Fig. 4)**. Tests on shive particles alone allow equilibrium to be reached relatively quickly at all RH levels for both adsorption and desorption, with no offset, indicating a reversible cycle. Conversely, the mass setting of the binder without the particles shows a ramp and has not reached equilibrium at 90 % RH **(Fig. 3b)**. This seems to confirm that the water quantity (40 % of the binder) is insufficient. Additionally, the compaction required to reach the target density of 1,300 $kg.m^{-3}$ could explain the less water availability and the resulting delay in carbonation. Formulation BP2_420 exhibits the same phenomenon from the 60 % RH level. This is the worst case explained by the combination of the highest proportion of binder (B/P=2) with the significant compaction needed to obtain 420 $kg.m^{-3}$ concrete **(Fig. 3c, red line)**. The resulting offset on desorption is the highest with 7.5 % of EMC at 0 % RH **(Fig. 4f)**. The proportion of binder in formulation BP1_478 is lower (B/P=1), which is beneficial regarding the amount of available water. However, such a small ratio means a high proportion of low-density particles, which required a very severe compaction likely to induce local drainage that explains an offset of approximately 2.5 % of water content. Consistently, this formulation did not reach the equilibrium from 75 % RH level **(Fig. 3c, green line)**. Finally, formulations BP1_379 and BP2_321 are those presenting the lowest offset values, below 2 % **(Fig. 4c,e)**. Formulation

BP1_379 required significant compaction for its manufacture but has a lower proportion of binder (B/P=1) favorable for water availability, and BP2_321 required almost no compaction. The LHC moisture contents obtained in this study are consistent with existing literature. At lower relative humidity (RH) levels (below 45%), the sorption capacity is less than 5% for all formulation, which aligns with findings from various studies [4,17,35]. However, at higher RH levels (≥70%), significant variations in moisture content are observed depending on the LHC formulation, reflecting the variability also reported in the literature due to differences in the formulation tested. For instance, Collet et al. [4] observed such variability when testing three different hemp-lime concrete formulations: sprayed, molded, and precast. They found that at higher RH levels, sprayed and molded hemp concretes exhibited similar mass changes, with water content reaching approximately 20% at 97% RH and irreversible mass changes around 5% after desorption. In contrast, precast hemp concrete showed water content peaking at around 44% at 97% RH and irreversible mass changes of about 2%. These differences were attributed to the higher hemp/binder ratio in precast concrete and the capillary condensation that occurs in the pore structure at high humidity, as well as possible lime carbonation.

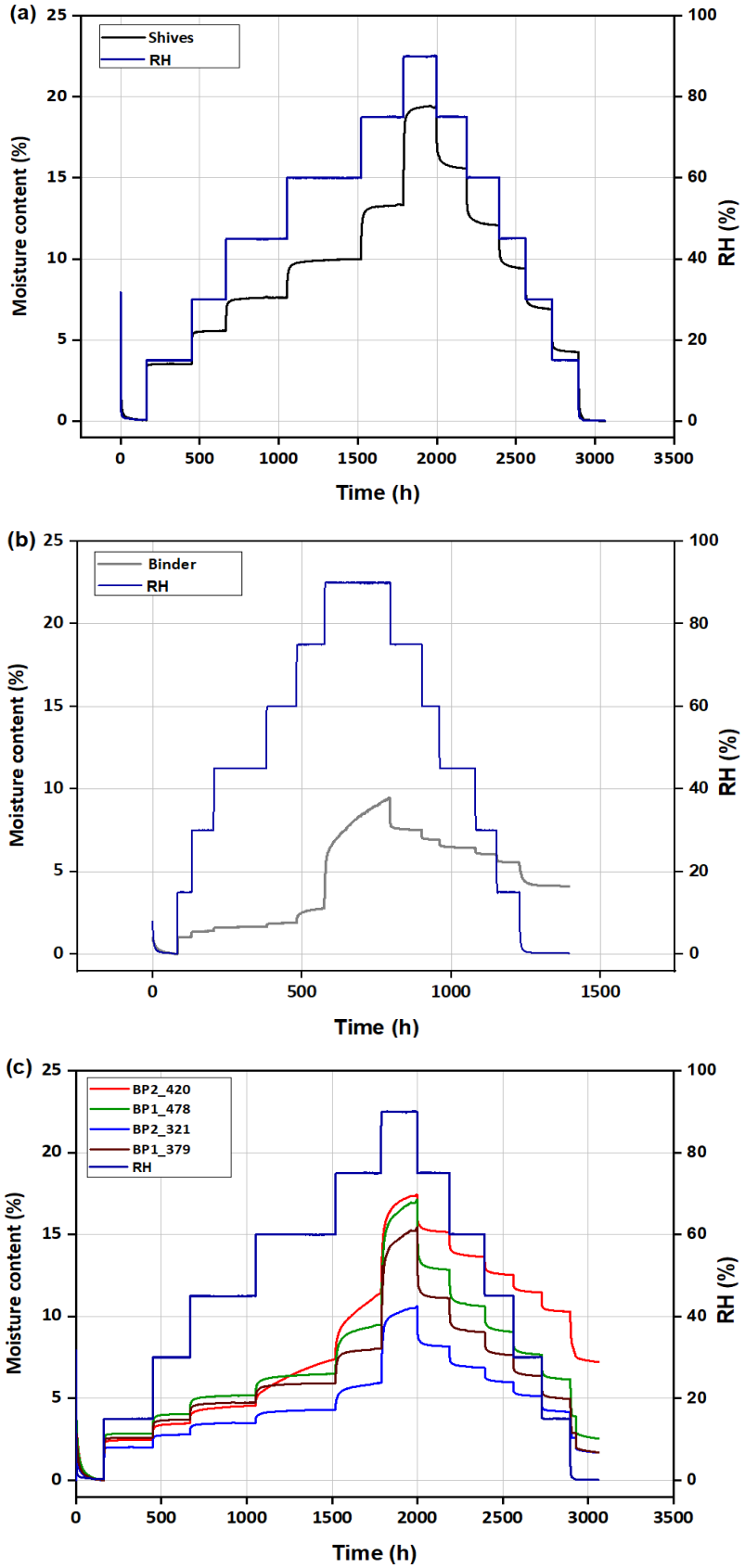

Fig. 3. Raw data from sorption tests: moisture content and relative humidity of the air over time for various materials: a) hemp shives, b) hydrated binder, c) Formulations BP1-379, BP1-478, BP2-321, and BP2-420.

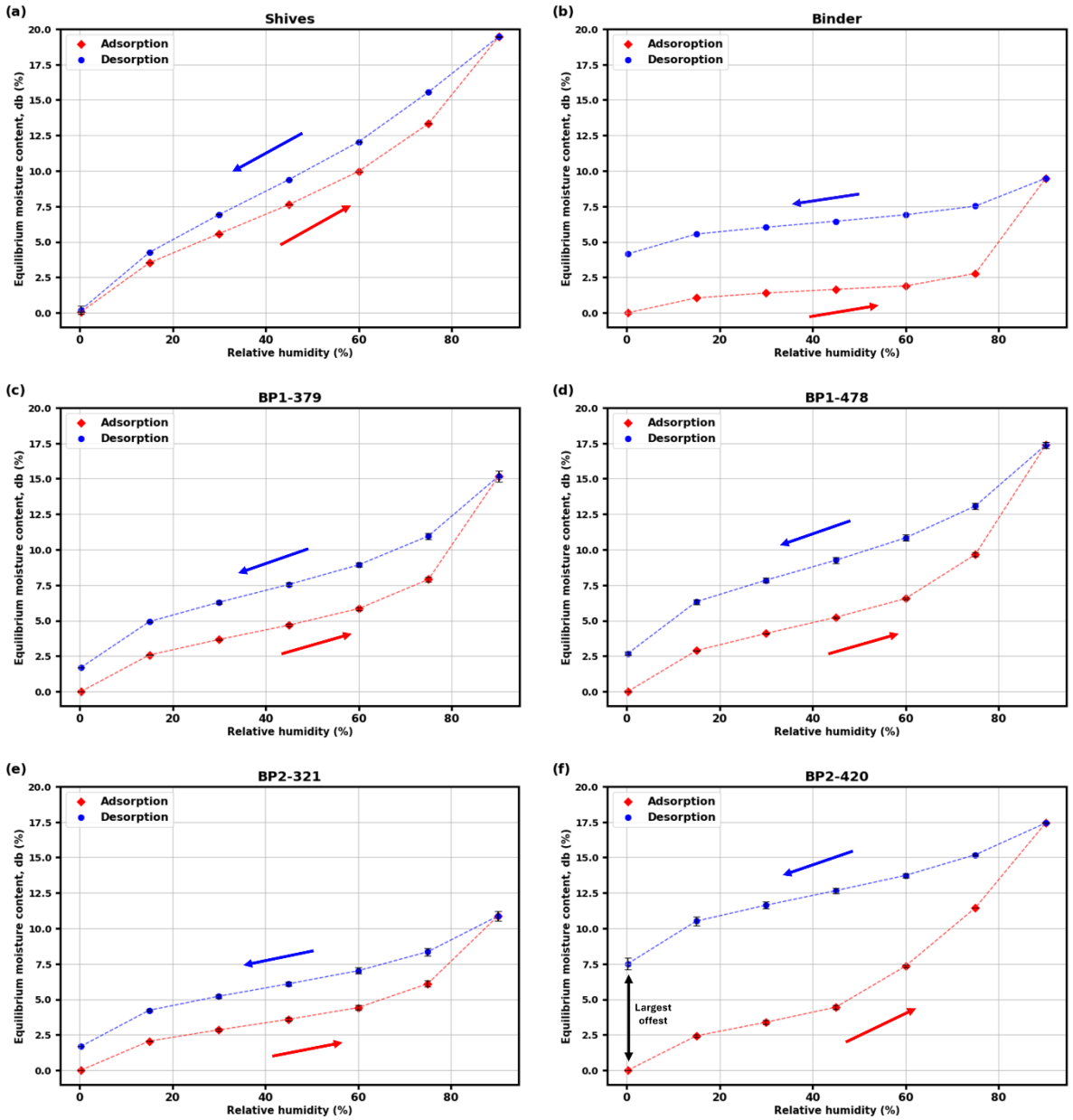

Fig. 4. Isotherm curves obtained (adsorption in red and desorption in blue) for : a) hemp shives, b) lime binder, c) BP1-379, d) BP1-478, e) BP2-321, and f) BP2-420. Standard deviations are included in the figures, but they are so small that the bars remain inside the markers.

3.2. Sorption behavior analyzed from the desorption data

The previous section proved that the adsorption data include an irreversible contribution added to the true, reversible, sorption behavior. These data are, therefore, unsuitable for analyzing pure sorption behavior. Conversely, the desorption curves, corrected for the offset, can be assumed to represent the pure sorption behavior. As explained in the material and methods, the

offset correction consists of using the final mass at the end of the complete sorption cycle as a reference dry mass. Consequently, all moisture contents were computed as the difference of actual mass minus the reference dry mass divided by the same reference dry mass.

The isothermal desorption curves **(Fig. 5)** reveal that sorption characteristics and capacities depend significantly on the sample. The sigmoid curves obtained for the different formulations are characteristic of a monolayer-multilayer sorption material (classification IUPAC type II isotherm). Hemp particles exhibit a high hygroscopicity, with an EMC of 13 % at 75 % RH. This is consistent with the hydrophilic nature of lignocellulosic biomass, namely due to the numerous hydroxyl groups in amorphous macromolecules [24,36,37]. On the contrary, instead of a distinctive “Point B” (inflection point at low RH values), the binder matrix exhibits a gradual curvature, which is an indication of a significant amount of overlap of monolayer coverage and the onset of multilayer adsorption [38]. The material's hygroscopicity is much lower, with an EMC of 2.6 % at 75 % RH. The various formulations tested show hygroscopicity values between these two extremes, reflecting a combination of the hemp's high sorption capacity and the binder's lower contribution.

To accurately describe the sorption behavior from desorption data, the GAB model was used to fit the desorption data **(Fig. 5)** for all materials. This model is widely recognized for its effectiveness in quantifying the moisture sorption properties of various materials. As already commented, some samples underwent chemical interactions between the vapor and the sample during adsorption, which fundamentally altered the physical state of the sample. Such interactions render the GAB model inapplicable for adsorption since it should apply to pure, reversible, sorption behavior. For this reason, the GAB parameters were not fitted for adsorption data.

The GAB model provided an excellent fit to the experimental data, as evidenced by the close agreement between observed data points and the fitted values **(Fig. 5)**. The quality of the fit is

assessed by the low error values of two objective indicators: the root mean square error (RMSE) and the sum of squared errors (SSE) **(Table 2)**.

These GAB parameters quantify the interaction between moisture and the material. The monolayer moisture content (MC_m), represents the moisture content at which bound water molecules are the most strongly held (availability of active sites for water sorption by the material), and the constants C and k are related to the heat of sorption for the first and subsequent layers of adsorbed water, respectively. When K approaches one, there is almost no distinction between multilayer molecules and liquid molecules (water molecules beyond the monolayer have the same characteristics as the molecules in the bulk liquid). In the present study, the mechanism of sorption is deduced from the combination of these parameters. The GAB parameters for binder (C = 39.3, K = 0.80, MC_m = 1.45%) in Table 2 illustrate the presence of a monolayer, with strongly bound water molecules and a multilayer, which has characteristics comparable with bulk liquid. Shives (C = 6.2, K = 0.62, MC_m = 9.68%) have more available active sites than binder, but water molecules are less strongly bound to the material and a more structured multilayer, where the water molecules are different from bulk liquid molecules. The mixed binder-shives (particles) materials show intermediate parameter values, reflecting the combined characteristics of the pure materials in the LHC formulations.

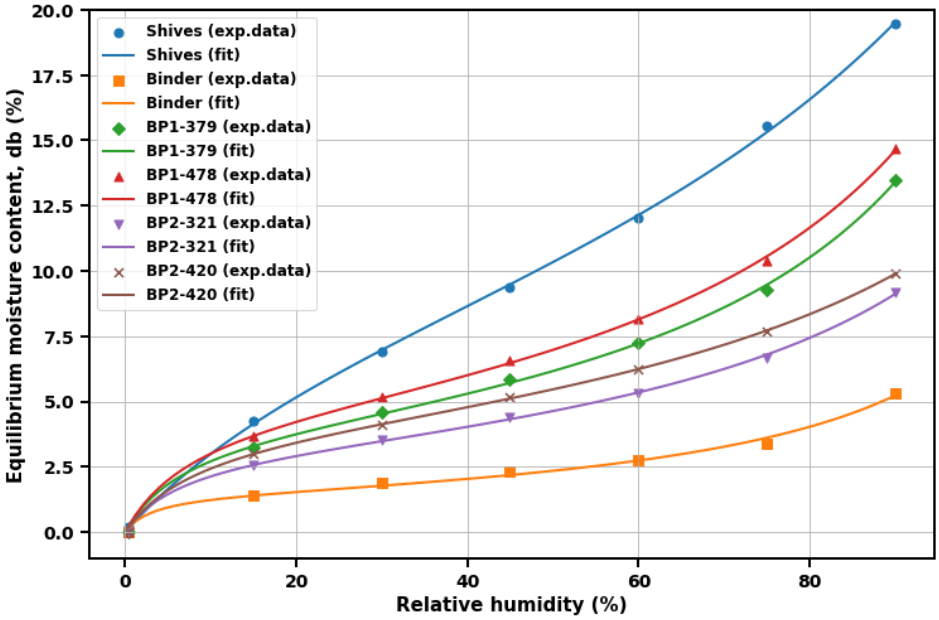

Fig. 5. Desorption isotherms, after offset correction, of the studied materials fitted by the GAB model (symbols: experimental values, continuous line: predicted values).

Table 2. Parameters of the GAB model fitted to the experimental desorption curves together with the quality criteria: Root mean square error (RMSE) and the sum of squared errors (SSE).

Constants	Desorption data					
	Shives	**Binder**	BP1-379	BP1-478	BP2-321	BP2-420
MC_m (%db)	***9.68***	***1.45***	4.07	4.73	3.18	4.02
k	***0.62***	***0.80***	0.78	0.76	0.73	0.68
C	***6.16***	***39.26***	18.74	17.20	20.66	17.86
RMSE	***0.12***	***0.13***	0.12	0.11	0.09	0.06
SSE	***0.11***	***0.11***	0.11	0.08	0.05	0.03

3.3.Rule of Mixtures applying GAB models

The GAB parameters for hemp shive particles and binders were used to predict the sorption behavior of formulations by the rule of mixtures (RoM). To do this, the EMC of both pure components are computed using the corresponding GAB models over the RH range and the EMC of the vegetable concrete is predicted as a weighted average of the mass ratio of the components. This allows the sorption curve of any vegetable concrete to be plotted. Its application in predicting the sorption isotherms of LHC mixtures has provided insightful data

(Fig. 6). This figure shows the moisture desorption behavior corrected by the offset value of the mixtures in comparison to their individual constituent hemp shives and hydrated binder. The experimental data were put together with the RoM predictions as markers for each specific mixture formulation, highlighting the interactions between the components.

The desorption isotherms for all formulations (BP1_379, BP1_478, BP2_321, and BP2_420) reveal that the RoM works quite well in predicting the equilibrium moisture content on average (**Fig. 6**). By removing the irreversible adsorption effects (offset), the experimental desorption isotherms align closely with the RoM predictions. In some cases, the experimental data almost perfectly overlay the theoretical curves, indicating that RoM is a reliable method for modeling these formulations. However, closer inspection reveals deviations from the RoM predictions, particularly for BP1_478, which exhibits the largest discrepancies. The experimental data for BP1_478 are substantially higher than the RoM predictions, especially at relative humidity levels above 60%, indicating that the RoM underestimates the moisture absorption capacity of this formulation. Keeping in mind that this configuration required the highest compaction level, leading to a reduction in pore size, consistent with the finding of Gourlay et al.[28], although the deviations remain limited in amplitude. Similarly, the experimental data for BP2_321 are slightly lower than the RoM predictions for a wide range of humidity levels (40-90%), indicating that the RoM overestimates the moisture uptake in this case, but with an error that remains less than -1 % (**Fig. 6c**). In contrast, BP1_379 shows experimental values very close to the RoM predictions, with deviations becoming noticeable only at higher humidity levels. Finally, BP2_420 demonstrates a strong alignment with the RoM, with minimal deviations, suggesting that the additivity assumption holds well for this formulation.

In conclusion, while the RoM provides a good approximation for most formulations, it struggles to fully capture the complexity of moisture absorption behaviors, particularly for BP1_478 at higher humidity levels, where a maximum error of 2.3% was observed between the predicted

and experimental values **(Fig. 6c)**. Nonetheless, for most cases, the sorption isotherms can be predicted with sufficient accuracy using the RoM combined with the GAB model, which is derived from the main constituents of the vegetal concrete, such as lime and hemp.

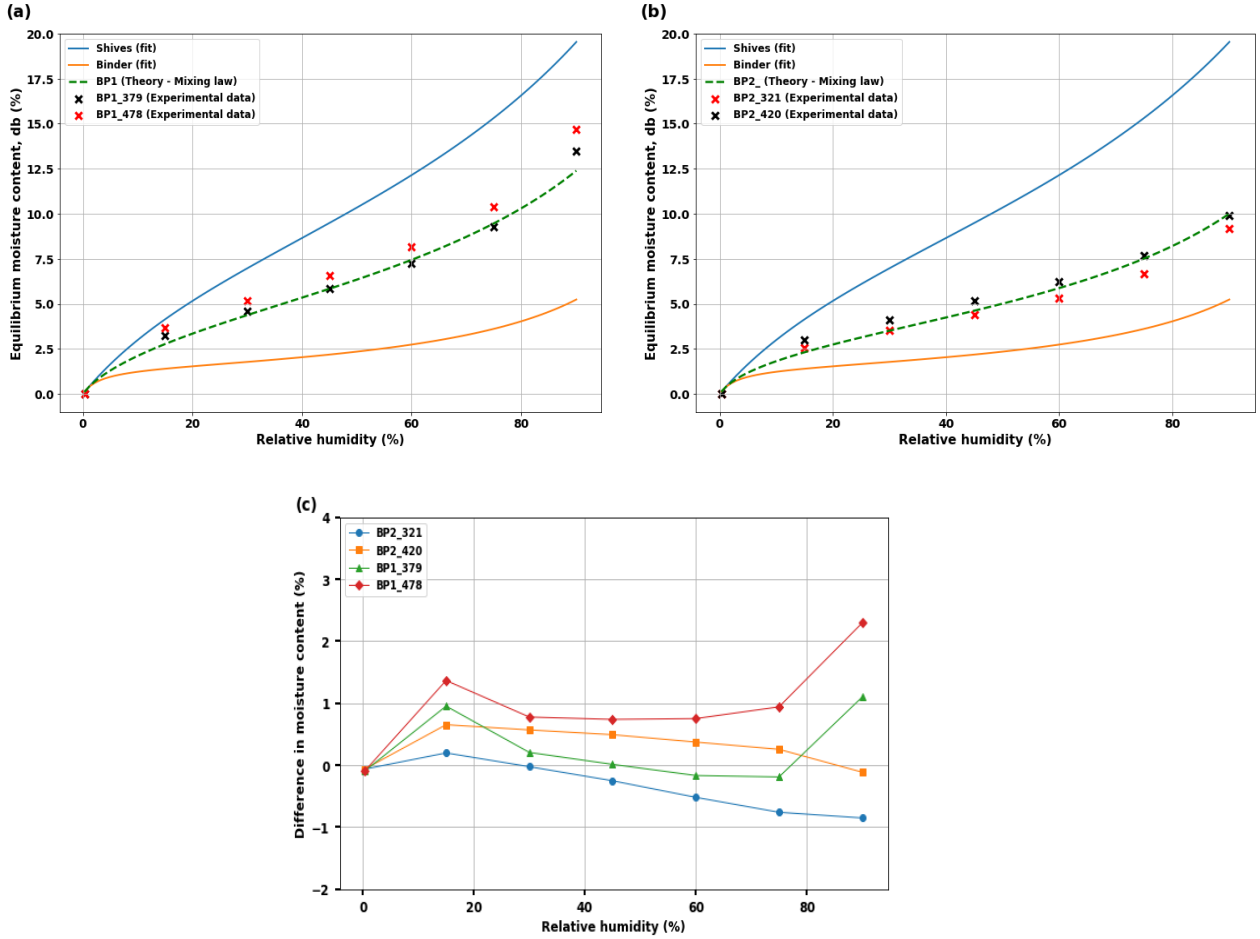

Fig. 6. Application of the rule of mixtures to the desorption isotherms of the studied materials. a) Formulations with a B/P ratio of 1, b) Formulations with a B/P ratio of 2, and c) The difference between the predicted data (obtained using the rule of mixtures) and the experimental data.

The long sorption tests applied in the present work, combined with our experimental design, suggest that the offset observed in some samples can be attributed to insufficient water availability during manufacture. It seems possible to improve the manufacture of LHC, with their complex mineral-vegetal interactions, by adding the necessary amount of water, which should vary according to the proportions of constituents and to the compaction level. Indeed, achieving the optimum setting is crucial for maximizing the concrete's mechanical strength,

which can only be attained when the binder has fully undergone hydration and carbonation reactions.

4. Conclusion

Lime-hemp concrete (LHC) represents a compelling research topic due to its low embodied energy, carbon sequestration potential, and natural thermal regulation. As a bio-based material, it offers promising solutions for sustainable and energy-efficient construction. This study provides a detailed investigation into the sorption behavior and isotherm characteristics of LHC, focusing on four formulations with varying binder/particle weight ratios (B/P = 1 and B/P = 2) and densities. Using Dynamic Vapor Sorption (DVS) measurements over a 3000-hour cycle, critical interactions between relative humidity (RH) and LHC components were uncovered, shedding light on its moisture behavior and potential for optimization. Key findings revealed that some formulations (e.g., BP2_420) failed to reach equilibrium during adsorption at RH levels above 60 %, leading to irreversible mass gain and offsets in the desorption phase. These issues were linked to insufficient water availability during fabrication, exacerbated by compaction and binder/particle ratios, which caused uneven water distribution due to drainage and reactivation of binder reactions under humid conditions. In contrast, desorption curves consistently reached equilibrium more rapidly across all RH levels, providing reliable data for further analysis and modeling. The Guggenheim-Anderson-de Boer (GAB) model was employed with success to fit with the experimental value. Finally, the rule of mixtures demonstrated effective predictability of hygroscopic behavior for all formulations, with a maximum error of 2.3% observed between the predicted and experimental values, primarily at high RH levels. The theoretical models applied in this study, including the GAB model and rule of mixtures, provide a robust framework for understanding the moisture behavior of LHC, and can thus be used to predict the sorption behavior of new formulations. The findings offer insights that can inform the refinement of fabrication processes, particularly in areas such as

binder/particle ratios, compaction methods, and water management, enhancing the material's performance and potential scalability in construction. Further investigations will concern the evaluation of the long-term performance of LHC under varying environmental conditions to better understand its durability and hygrothermal behavior in real-world scenarios.

Author contributions

Brahim Mazian: Conceptualization; Methodology; Software; Validation; Formal analysis; Investigation; Data Curation; Writing – Original Draft; Visualization.

Giana Almeida: Conceptualization; Methodology; Formal analysis; Validation; Data Curation; Writing - Review & Editing; Supervision.

Nils Frantz: Conceptualization; Methodology; Investigation.

Patrick Perré: Conceptualization; Methodology; Formal analysis; Data Curation; Writing - Review & Editing; Supervision; Project administration; Funding acquisition.

Author ORCID

Brahim Mazian: https://orcid.org/0000-0001-7459-0195

Giana Almeida: https://orcid.org/0000-0002-8413-8677

Nils Frantz:

Patrick Perré: https://orcid.org/0000-0003-0419-4810

Acknowledgments

Communauté urbaine du Grand Reims, Département de la Marne, Région Grand Est and European Union (FEDER Champagne–Ardenne 2014–2020, FEDER Grand Est 2021–2027) are acknowledged for their financial support to the Chair of Biotechnology of CentraleSupélec and the Centre Européen de Biotechnologie et de Bioéconomie (CEBB).

References

[1] A.S. Ahmad, M.Y. Hassan, M.P. Abdullah, H.A. Rahman, F. Hussin, H. Abdullah, R. Saidur, A review on applications of ANN and SVM for building electrical energy consumption forecasting, Renewable and Sustainable Energy Reviews 33 (2014) 102–109. https://doi.org/10.1016/j.rser.2014.01.069.

[2] K. Amasyali, N.M. El-Gohary, A review of data-driven building energy consumption prediction studies, Renewable and Sustainable Energy Reviews 81 (2018) 1192–1205. https://doi.org/10.1016/j.rser.2017.04.095

[3] B. Mazian, E. Wirquin, K. Aguibi, P. Martin, L. Chaveriat, V. Dubois, Effect of mixing conditions on the density, morphology, thermal and mechanical properties of mineral foam, Journal of Building Engineering 52 (2022) 104410. https://doi.org/10.1016/j.jobe.2022.104410

[4] F. Collet, J. Chamoin, S. Pretot, C. Lanos, Comparison of the hygric behaviour of three hemp concretes, Energy and Buildings 62 (2013) 294–303. https://doi.org/10.1016/j.enbuild.2013.03.010.

[5] Y.X. Chen, F. Wu, Q. Yu, H.J.H. Brouwers, Bio-based ultra-lightweight concrete applying miscanthus fibers: Acoustic absorption and thermal insulation, Cement and Concrete Composites 114 (2020) 103829. https://doi.org/10.1016/j.cemconcomp.2020.103829.

[6] O. Onuaguluchi, N. Banthia, Plant-based natural fibre reinforced cement composites: A review, Cement and Concrete Composites 68 (2016) 96–108. https://doi.org/10.1016/j.cemconcomp.2016.02.014.

[7] Y. Hustache, L. Arnaud, Synthèse Des Connaissances Sur Les Bétons et Mortiers de Chanvre, Construire En Chanvre (2008).

[8] P. Tronet, T. Lecompte, V. Picandet, C. Baley, Study of lime hemp concrete (LHC) – Mix design, casting process and mechanical behaviour, Cement and Concrete Composites 67 (2016) 60–72. https://doi.org/10.1016/j.cemconcomp.2015.12.004.

[9] S. Barbhuiya, B. Bhusan Das, A comprehensive review on the use of hemp in concrete, Construction and Building Materials 341 (2022) 127857. https://doi.org/10.1016/j.conbuildmat.2022.127857.

[10] M. Lawrence, P. Walker, Enrico, Fodde, Kevin, Paine, Hygrothermal performance of an experimental hemp–lime building, Construction and Building Materials 36 (2012) 270–275. https://doi.org/10.1016/j.conbuildmat.2012.04.123.

[11] N. Frantz, L.F. Dutra, D.M. Nguyen, G. Almeida, P. Perré, Effects of phase ratios, density and particle shapes on directional thermal conductivity of vegetable concrete: A predictive model, Construction and Building Materials 410 (2024) 134238. https://doi.org/10.1016/j.conbuildmat.2023.134238.

[12] F. Collet, S. Pretot, Thermal conductivity of hemp concretes: Variation with formulation, density and water content, Construction and Building Materials 65 (2014) 612–619. https://doi.org/10.1016/j.conbuildmat.2014.05.039.

[13] T. Jami, S.R. Karade, L.P. Singh, A review of the properties of hemp concrete for green building applications, Journal of Cleaner Production 239 (2019) 117852. https://doi.org/10.1016/j.jclepro.2019.117852.

[14] Y. Aït Oumeziane, M. Bart, S. Moissette, C. Lanos, Hysteretic Behaviour and Moisture Buffering of Hemp Concrete, Transp Porous Med 103 (2014) 515–533. https://doi.org/10.1007/s11242-014-0314-7.

[15] B. Mazhoud, F. Collet, S. Pretot, J. Chamoin, Hygric and thermal properties of hemp-lime plasters, Building and Environment 96 (2016) 206–216. https://doi.org/10.1016/j.buildenv.2015.11.013.

[16] M. Asli, F. Brachelet, E. Sassine, E. Antczak, Thermal and hygroscopic study of hemp concrete in real ambient conditions, Journal of Building Engineering 44 (2021) 102612. https://doi.org/10.1016/j.jobe.2021.102612.

[17] B. Seng, C. Magniont, S. Lorente, Characterization of a precast hemp concrete block. Part II: Hygric properties, Journal of Building Engineering 24 (2019) 100579. https://doi.org/10.1016/j.jobe.2018.09.007.

[18] R. Walker, S. Pavía, Moisture transfer and thermal properties of hemp–lime concretes, Construction and Building Materials 64 (2014) 270–276. https://doi.org/10.1016/j.conbuildmat.2014.04.081.

[19] K. Abahri, R. Belarbi, C.E. Hachem, Caractérisation macro-hydriques des matériaux biosourcés, (2015).

[20] Afnor, NF EN ISO 12571, Afnor EDITIONS (2013). https://m.boutique.afnor.org/fr-fr/norme/nf-en-iso-12571/performance-hygrothermique-des-materiaux-et-produits-pour-le-batiment-deter/fa177734/42249 (accessed April 12, 2024).

[21] F. Benmahiddine, F. Bennai, R. Cherif, R. Belarbi, A. Tahakourt, K. Abahri, Experimental investigation on the influence of immersion/drying cycles on the hygrothermal and mechanical properties of hemp concrete, Journal of Building Engineering 32 (2020) 101758. https://doi.org/10.1016/j.jobe.2020.101758.

[22] E. Latif, M. Lawrence, A. Shea, P. Walker, Moisture buffer potential of experimental wall assemblies incorporating formulated hemp-lime, Building and Environment 93 (2015) 199–209. https://doi.org/10.1016/j.buildenv.2015.07.011.

[23] F. Collet, M. Bart, L. Serres, J. Miriel, Porous Structure and Water Vapour Sorption of Hemp-Based Materials, Construction and Building Materials 22 (2008) 1271–1280. https://doi.org/10.1016/j.conbuildmat.2007.01.018.

[24] G. Almeida, R. Rémond, P. Perré, Hygroscopic behaviour of lignocellulosic materials: Dataset at oscillating relative humidity variations, Journal of Building Engineering 19 (2018) 320–333. https://doi.org/10.1016/j.jobe.2018.05.005.

[25] B. Djolani, Hystérèse et effets de second ordre de la sorption d'humidité dans le bois aux températures de 5°, 21°, 35°, 50° C, Ann. Sci. Forest. 29 (1972) 465–474. https://doi.org/10.1051/forest/19720404.

561 [26] G. Almeida, R.E. Hernández, Influence of the pore structure of wood on moisture
562 desorption at high relative humidities, Wood Material Science & Engineering 2 (2007)
563 33–44. https://doi.org/10.1080/17480270701538383.

564 [27] A. Fabbri, F. McGregor, Impact of the determination of the sorption-desorption curves on
565 the prediction of the hemp concrete hygrothermal behaviour, Construction and Building
566 Materials 157 (2017) 108–116. https://doi.org/10.1016/j.conbuildmat.2017.09.077.

567 [28] E. Gourlay, P. Glé, S. Marceau, C. Foy, S. Moscardelli, Effect of water content on the
568 acoustical and thermal properties of hemp concretes, Construction and Building Materials
569 139 (2017) 513–523. https://doi.org/10.1016/j.conbuildmat.2016.11.018.

570 [29] H. Derluyn, D. Derome, J. Carmeliet, E. Stora, R. Barbarulo, Hysteretic moisture behavior
571 of concrete: Modeling and analysis, Cement and Concrete Research 42 (2012) 1379–1388.
572 https://doi.org/10.1016/j.cemconres.2012.06.010.

573 [30] F. Benmahiddine, F. Bennai, A. Charaka, A.E.A. Hamami, A. Tahakourt, R. Belarbi,
574 Multi-scale analysis of the effects of hysteresis on the hydrothermal behaviour of bio-
575 based materials: Application to hemp concrete, Construction and Building Materials 411
576 (2024) 134107. https://doi.org/10.1016/j.conbuildmat.2023.134107.

577 [31] R. Rémond, G. Almeida, P. Perré, The gripped-box model: A simple and robust
578 formulation of sorption hysteresis for lignocellulosic materials, Construction and Building
579 Materials 170 (2018) 716–724. https://doi.org/10.1016/j.conbuildmat.2018.02.116.

580 [32] N. Holcroft, A. Shea, Effect of compaction on moisture buffering of hemp-lime insulation,
581 Academic Journal of Civil Engineering (2015) 542-546.
582 https://doi.org/10.26168/icbbm2015.84.

583 [33] J.I. Alvarez, R. Veiga, S. Martínez-Ramírez, M. Secco, P. Faria, P.N. Maravelaki, M.
584 Ramesh, I. Papayianni, J. Válek, RILEM TC 277-LHS report: a review on the mechanisms
585 of setting and hardening of lime-based binding systems, Mater Struct 54 (2021) 63.
586 https://doi.org/10.1617/s11527-021-01648-3.

587 [34] P. Guiraud, Fabrication du ciment et empreinte CO2, Infociments (2020).
588 https://www.infociments.fr/enjeux-societe/la-fabrication-du-ciment-source-maitrisee-de-
589 co2 (accessed September 21, 2023).

590 [35] M. Rahim, O. Douzane, A.D. Tran Le, G. Promis, B. Laidoudi, A. Crigny, B. Dupre, T.
591 Langlet, Characterization of flax lime and hemp lime concretes: Hygric properties and
592 moisture buffer capacity, Energy and Buildings 88 (2015) 91–99.
593 https://doi.org/10.1016/j.enbuild.2014.11.043.

594 [36] S. Alix, E. Philippe, A. Bessadok, L. Lebrun, C. Morvan, S. Marais, Effect of chemical
595 treatments on water sorption and mechanical properties of flax fibres, Bioresource
596 Technology 100 (2009) 4742–4749. https://doi.org/10.1016/j.biortech.2009.04.067.

597 [37] C. Simón, L.G. Esteban, P. de Palacios, F.G. Fernández, A. García-Iruela, Thermodynamic
598 properties of the water sorption isotherms of wood of limba (Terminalia superba Engl. &
599 Diels), obeche (Triplochiton scleroxylon K. Schum.), radiata pine (Pinus radiata D. Don)
600 and chestnut (Castanea sativa Mill.), Industrial Crops and Products 94 (2016) 122–131.
601 https://doi.org/10.1016/j.indcrop.2016.08.008.

602 [38] M. Thommes, K. Kaneko, A.V. Neimark, J.P. Olivier, F. Rodriguez-Reinoso, J. Rouquerol,
603 K.S.W. Sing, Physisorption of gases, with special reference to the evaluation of surface
604 area and pore size distribution (IUPAC Technical Report), Pure and Applied Chemistry 87
605 (2015) 1051–1069. https://doi.org/10.1515/pac-2014-1117.

606